Striatal tau burden is increased in APOE-e4+ mild cognitive impairment

Jason Langley[1], Sumanth Dara[2], Ilana J. Bennett[3], and Xiaoping P. Hu[1,2] for the Alzheimer's Disease Neuroimaging Initiative

[1] Center for Advanced Neuroimaging, University of California Riverside, Riverside, CA, USA
[2] Department of Bioengineering, University of California Riverside, Riverside, CA, USA
[3] Department of Psychology, University of California Riverside, Riverside, CA, USA

E-mail: xhu ,at' engr.ucr.edu

Abstract

Background: The presence of β-amyloid (Aβ) extracellular plaques and hyper-phosphorylated tau neurofibrillary tangles characterize the pathology of Alzheimer's disease (AD) and mild cognitive impairment (MCI). Individuals carrying the apolipoprotein E-ε4 (APOE-ε4) allele are at increased risk of cognitive decline and developing AD pathology. The ^{18}F-AV1451 radioligand allows for assessment of tau burden *in vivo*. However, this radioligand also binds with iron and this off-target binding can occlude tau deposition in iron rich gray matter structures such as the putamen and caudate nucleus.

Methods: We employ a MRI measure sensitive to iron, quantitative susceptibility mapping, to control for off-target binding effects of the ^{18}F-AV1451 radioligand and examine tau burden in the striatum. 20 APOE-ε4 negative MCI, 20 APOE-ε4 positive MCI, and 29 APOE-ε4 negative control participants from ADNI were used in this analysis.

Results: Increased tau pathology (^{18}F-AV1451 PET uptake), after controlling for tissue susceptibility, was found in the putamen and caudate nucleus of APOE-ε4+ MCI participants as compared to APOE-ε4 negative MCI and control participants. Tau burden in the caudate nucleus of the APOE-ε4+ MCI group was correlated with Montreal Cognitive Assessment (MOCA) score with higher caudate tau burden associated with greater cognitive impairment.

Conclusions: Controlling for iron allows for the assessment of tau burden in iron rich deep gray matter structures. Our findings suggest that APOE-ε4 allele increases the risk of developing AD pathology in the striatum.

Keywords: Mild Cognitive Impairment, Alzheimer's Disease, ^{18}F-AV1451 PET, quantitative susceptibility mapping

1. Introduction

Patients with mild cognitive impairment (MCI) exhibit declines in cognitive performance that do not meet the threshold for dementia, but are likely to later convert to Alzheimer's disease (AD).[1] Individuals carrying the apolipoprotein E-ε4 (APOE-ε4) allele are at increased risk of cognitive decline and developing AD pathology.[2] AD and MCI pathology is characterized by the presence of β-amyloid (Aβ) extracellular plaques and neurofibrillary tangles containing hyper-phosphorylated tau.[3] Tau deposition can be assessed using the radioligand ^{18}F-AV1451 (tau-PET), which is known to bind with iron in addition to tau NFTs.[4]

Cortical tau-PET uptake is associated with MRI measures sensitive to iron.[5] This off-target binding obstructs measurement of tau burden in iron-rich deep gray matter structures, like those that comprise the striatum. Postmortem studies of AD patients have reported the presence of NFTs in the striatum[6,7] and striatal Aβ load is associated with AD-related cognitive decline.[8–10] However, *in vivo* examination of striatal NFTs in MCI and the impact of APOE-ε4 carrier status remain unexplored due to off-target binding effects. We use quantitative susceptibility mapping (QSM) to quantify iron and remove iron-related off-target binding effects in the striatum and examine striatal tau burden in APOE-ε4 positive (i.e. one or more APOE-ε4 alleles) MCI, APOE-ε4 negative MCI, and APOE-ε4 negative control participants.

2. Methods

2.1 ADNI Overview

Data used in this study were obtained from the ADNI database (adni.loni.usc.edu). ADNI was launched in 2003 as a public-private partnership supported project. The ADNI was launched in 2003 as a public-private partnership, led by Principal Investigator Michael W. Weiner, MD. The primary goal of ADNI is to test whether serial MRI, PET, other biological markers, and clinical and neuropsychological

assessments can be combined to measure the progression of MCI and early AD. Up-to-date information can be found at www.adni-info.org. The ADNI data were collected from over 50 research sites and the ADNI study was approved by the local Institutional Review Boards (IRBs) of all participating sites. The detailed information and complete list of ADNI sites' IRBs could be found at http://adni.loni.usc.edu/about/centers-cores/study-sites/ and http://www.adni-info.org/.

Study subjects and, if applicable, their legal representatives, gave written informed consent at the time of enrollment for imaging data, genetic sample collection and clinical questionnaires. Exclusion criteria determined by ADNI was followed. Subjects were excluded from the analysis if they had Parkinson's disease, Huntington's disease, progressive supranuclear palsy, a history of seizures, normal pressure hydrocephalus, brain tumors, multiple sclerosis, subdural hematoma, a history of head trauma, known brain structural abnormalities, a history of major depression, schizophrenia, alcohol or substance abuse, bipolar disorder, or currently using psychoactive medications. Individuals with contraindications to MRI imaging such as pacemakers, heart valves, or other foreign objects or implants in the body were excluded.

2.2 Participants

The ADNI3 database was queried for individuals with tau-sensitive PET (^{18}F-AV1451), T_1-weighted, and multi-echo gradient echo MRI images at the same scanning visit, as well as APOE-ε4 status. Participants with either one or two APOE-ε4 alleles were considered APOE-ε4 positive. From this cohort, we selected all individuals with a diagnostic status of MCI or control at the time of the visit, which included 20 APOE-ε4 negative (ε4-) and 20 APOE-ε4 positive (ε4+) MCI participants and 29 APOE-ε4- control participants. Alzheimer's Disease Assessment Scale cog-13 (ADAS13) and Montreal Cognitive Assessment (MOCA) score were downloaded for each subject. Details regarding image acquisition parameters can be found at www.adni-info.org/methods. Imaging data were downloaded in December 2019.

All MCI participants in the ADNI3 database had a subjective memory concern reported by a clinician, abnormal memory function on the education-adjusted Logical Memory II subscale, and a clinical dementia rating greater than 0.5. Further, MCI participants were deemed to have cognitive and functional performance that was sufficiently intact to not merit a diagnosis of attention deficit disorder by the site physician.

2.3 MRI Acquisition

All MRI data used in this study were acquired on Siemens Prisma or Prisma fit scanners. Anatomic images were acquired with an MP-RAGE sequence (echo time (TE)/repetition time (TR)/inversion time=2.98/2300/900 ms, flip angle=9°, voxel size=1.0×1.0×1.0 mm^3, and GRAPPA acceleration factor=2) and were used for registration to common space and correction of partial volume effects in the PET data.

Iron-sensitive data were collected with a three-echo 2D gradient recalled echo (GRE) sequence ($TE_1/\Delta TE/TR$ = 6/7/650 ms, flip angle=20°, field of view=220×220 mm^2, matrix size of 256×256, 44 slices, slice thickness=4.0 mm) and used for measurement of brain iron.

2.4 QSM Processing

Susceptibility images were constructed from the 2D GRE images. A brain mask was derived from the first echo of the magnitude data. Background phase was removed using harmonic phase removal using the Laplacian operator (iHARPERELLA).[11] Susceptibility maps were then derived from the frequency map of brain tissue using an improved least-squares (iLSQR) method and Laplace filtering with a threshold of 0.04 as a truncation value. All susceptibility images were processed in MATLAB (The MathWorks, Inc., Natick, MA, USA). The resulting susceptibility maps were aligned to each subject's T_1-weighted image using a rigid body transform derived via the magnitude image from the first echo with the T_1-weighted image. Susceptibility values were normalized to median susceptibility in the lateral ventricles.

2.5 PET Acquisition and Processing

The radiochemical synthesis of ^{18}F-AV1451 was overseen and regulated by Avid Radiopharmaceuticals and distributed to the qualifying ADNI sites where PET imaging was performed according to standardized protocols. The ^{18}F-AV-1451 protocol entailed the injection of 10 mCi of tracer followed by an uptake phase of 80 min during which the subjects remained out of the scanner, and then collection of the ^{18}F-AV-1451 emission data as 4×5min frames. PET with computed tomography imaging (PET/CT) scans preceded these acquisitions with a CT scan for attenuation correction; PET-only scanners performed a transmission scan following the emission scan.

PET imaging data were analyzed with FSL and PET partial volume correction (PETPVC) toolbox [12]. Motion was corrected in ^{18}F-AV1451 PET scans were co-registered to the first frame and averaged using rigid-body transforms with FLIRT in FSL. Next, the motion-corrected mean PET scans were registered to the participant's own T_1-weighted MRI image using a rigid-body transform with a normalized mutual information cost function in FLIRT. Grey matter, white matter, and CSF maps were segmented in the T_1-weighted MRI image and used to correct for partial volume effects using PETPVC.[12] A combination of Labbé[13] and region-based voxel-wise correction[14] was chosen to mitigate

	Control	MCI		*F*
		APOE-ε4-	APOE-ε4+	
N (M/F)	29 (13/16)	20 (11/9)	20 (13/7)	<3.086
Age	73.7±1.5	75.6±1.8	74.4±1.9	1.479
Education	16.3±0.5	15.6±0.6	15.4±0.6	1.105
MOCA	24.7±0.6	21.9±0.8	20.7±0.8	**8.986**
CDR	0.0±0.0	0.5±0.0	0.5±0.0	**186.746**
ADAS13	13.7±0.9	16.8±1.2	21.4±1.4	**16.453**

Table 1. Demographic information for the groups used in this analysis. Data is presented as mean ± standard error. One-way analysis of variances (ANOVAs) were used for group comparisons of age, education, and cognition from which *F* values are shown. Bold *F* values indicate significant comparisons. MoCA = Montreal cognitive assessment; MMSE = Mini-Mental State Exam. CDR = clinical dementia rating, ADAS = Alzheimer's Disease Assessment Scale, APOE = Apolipoprotein E ε4 allele

sensitivity to point spread function mismatch. The median standardized uptake value (SUV) in left + right cerebellar cortex was chosen as a reference. Figure 1 shows a comparison of typical susceptibility maps and SUV ratios (SUVR) for a subject from each group.

2.6 Regions of Interest

The Harvard-Oxford subcortical atlas was used to define standard space regions of interest (ROIs) in bilateral putamen and caudate. The ROIs were then transformed from MNI space to subject space using nonlinear transforms in FSL as described in the earlier work[15] and linear transforms derived in previous sections. Once in subject space, each aligned ROI was thresholded at 60% and binarized. Mean susceptibility and tau-PET SUVR were measured in each resultant ROI for each participant.

2.7 Statistical Analysis

All statistical analyses were performed using IBM SPSS Statistics software version 24 (IBM Corporation, Somers, NY, USA) and results are reported as mean ± standard error. A *P* value of 0.05 was considered significant for all statistical tests performed in this work. Normality of tau-PET and iron data was assessed using the Shapiro-Wilk test for each group and all data was found to be normal. The relationship between tau-PET SUVR and iron in striatal ROIs was assessed by Pearson correlations in each ROI. The effect of group (APOE-ε4+ MCI, APOE-ε4- MCI, control) was tested with separate analysis of covariance (ANCOVA) in each ROI (putamen, caudate nucleus) for tau-PET SUVR, controlling for sex and iron. For all ANCOVAs, if the interaction was significant, post hoc comparisons between each pair of groups were performed using respective two-tailed t-tests. As striatal Aβ burden is associated with AD-related cognitive decline,[8-10] we elected to examine the effect of striatal tau burden on general cognition by correlating striatal tau-PET SUVR with general cognitive measures, controlling for susceptibility.

3. Results

3.1 Sample Demographics

Demographic data for each group is shown in Table 1. No significant group effect was seen for age (P=0.234; F=1.479), education (P=0.367; F=1.105), or gender (Ps>0.079; Fs<3.086). Significant group effects were seen for all cognitive measures with MOCA ($P<10^{-4}$; F=8.986), CDR ($P<10^{-4}$; F=186.746), and ADAS13 ($P<10^{-4}$; F=16.453). Both MCI groups showed reduced scores on MOCA (APOE-ε4+: P=0.0002; APOE-ε4-: P=0.005) and CDR (APOE-ε4+: $P<10^{-4}$; APOE-ε4-: $P<10^{-4}$) relative to the control group. Higher ADAS13 scores, indicating greater cognitive impairment, were seen in the APOE-ε4+ MCI group relative to the APOE-ε4- MCI (P=0.001) and control ($P<10^{-4}$) groups, and in the APOE-ε4- MCI group relative to controls (P=0.037).

3.2 Relationships Between Tau-PET and Susceptibility

The effect of group (APOE-ε4+ MCI, APOE-ε4- MCI, control) was tested with separate analysis of variance (ANOVAs) in each striatal region. No significant main effect in group was seen in putamen (P=0.309; F=1.195) or caudate (P=0.083; F=2.585) susceptibility. Significant correlations between striatal tau-PET SUVR and susceptibility were observed for each group in caudate (control: r=0.520, P=0.005; ε4-: r=0.857, $P<10^{-3}$; ε4+: r=0.681, P=0.002) and putamen (control: r=0.628, P=0.002; ε4-: r=0.522, P=0.034; ε4+: r=0.532, P=0.028).

3.3 APOE Group Differences in Tau-PET

The effect of group was tested with separate ANCOVAs in each striatal ROI, controlling for susceptibility (see Figure 1). For putamen, there was a significant main effect in group ($P<10^{-4}$; F=10.597). Pairwise-comparisons of the marginal

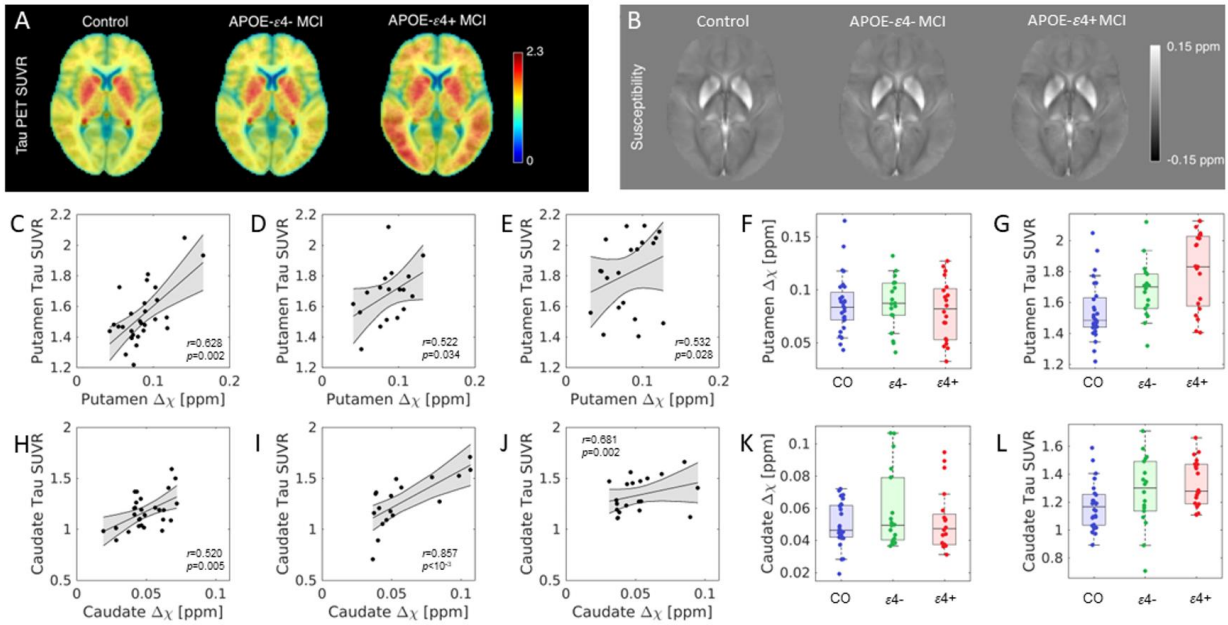

Figure 1. Mean tau-pet SUVR and mean susceptibility images at the level of the striatum in control, APOE-ε4- MCI, and APOE-ε4+ MCI groups are displayed in (A) and (B), respectively. Correlations between susceptibility and tau-PET SUVR in the putamen for control, APOE-ε4- MCI, and APOE-ε4+ MCI groups are shown in (C), (D), and (E), respectively. (F) and (G) show group comparisons for putamen susceptibility and putamen tau-PET SUVR, respectively. Correlations between susceptibility and tau-PET SUVR in the caudate nucleus for control, APOE-ε4- MCI, and APOE-ε4+ MCI groups are shown in (H), (I), and (J), respectively. (K) and (L) show group comparisons for susceptibility and tau-PET SUVR in the caudate nucleus, respectively.

means showed higher putamen tau-PET SUVR in APOE-ε4+ MCI relative to APOE-ε4- MCI (P=0.023) and control (P<10^{-3}) groups. Putamen tau-PET SUVR was higher in the APOE-ε4- MCI group relative to the control group (P=0.047). A significant main effect in group was seen in caudate nucleus (P=0.013; F=4.634). Comparison of marginal means showed elevated caudate tau-PET SUVR in APOE-ε4+ MCI relative to APOE-ε4- MCI (P=0.046) and control (P=0.008) groups. No difference was seen in caudate tau-PET SUVR between APOE-ε4- MCI and control groups (P=0.352).

3.4 Relationships to Cognition

A significant correlation was seen between tau-PET SUVR and MOCA in the caudate of the APOE-ε4+ MCI group (r=-0.713; P=0.004). No significant correlation was seen between caudate tau-PET SUVR and MOCA in the APOE-ε4- MCI and control groups (Ps>0.173). No significant correlation was seen between ADAS13 score and caudate tau-PET SUVR for any group (Ps>0.898). No significant correlation was seen between putamen tau-PET SUVR and either cognitive measure in any group (Ps>0.370).

3. Discussion

Iron is an off-target bind for the ^{18}F-AV1451 radioligand and, in iron rich gray matter structures, this off-target binding will contribute to radioligand uptake. This study uses susceptibility, a MRI measure sensitive to iron deposition, to control for off-target binding effects associated with the ^{18}F-AV1451 radioligand and examine tau burden in iron-rich gray matter nuclei in relation to APOE-ε4 carrier status. Elevated tau-PET SUVR was observed in the putamen and caudate nucleus of the APOE-ε4+ group relative to APOE-ε4- and control groups. These observations agree with human stem cell models where expression of the APOE-ε4 allele is linked with increased tau pathology[16] and histological studies that found tau NFTs in the striatum.[6,7]

Interestingly, caudate tau-PET SUVR was significantly correlated to MOCA in the APOE-ε4+ group with higher tau burden related to lower cognitive scores (lower MOCA scores). While, this data does not provide information to Aβ load in the striatum, this result agrees with observations relating higher striatal Aβ SUVR to decreased cognitive scores.[8-10] However, these results should be interpreted with caution given the complexity of cognition and the small number of subjects in this analysis. Taken together, these

findings suggest that APOE-ε4 allele increases the risk of developing AD pathology in the striatum.

Acknowledgements

Data used in preparation of this article were obtained from the Alzheimer's Disease Neuroimaging Initiative (ADNI) database (adni.loni.usc.edu). As such, the investigators within the ADNI contributed to the design and implementation of ADNI and/or provided data but did not participate in analysis or writing of this report. A complete listing of ADNI investigators can be found at: http://adni.loni.usc.edu/wp-content/uploads/how_to_apply/ADNI_Acknowledgement_List.pdf

References

1. Albert, M.S., *et al.* The diagnosis of mild cognitive impairment due to Alzheimer's disease: recommendations from the National Institute on Aging-Alzheimer's Association workgroups on diagnostic guidelines for Alzheimer's disease. *Alzheimers Dement* **7**, 270-279 (2011).

2. Roses, A.D. & Saunders, A.M. APOE is a major susceptibility gene for Alzheimer's disease. *Curr Opin Biotechnol* **5**, 663-667 (1994).

3. Hardy, J. & Allsop, D. Amyloid deposition as the central event in the aetiology of Alzheimer's disease. *Trends Pharmacol Sci* **12**, 383-388 (1991).

4. Lowe, V.J., *et al.* An autoradiographic evaluation of AV-1451 Tau PET in dementia. *Acta Neuropathol Commun* **4**, 58 (2016).

5. Spotorno, N., *et al.* Relationship between cortical iron and tau aggregation in Alzheimer's disease. *Brain* **143**, 1341-1349 (2020).

6. Braak, H. & Braak, E. Alzheimer's disease: striatal amyloid deposits and neurofibrillary changes. *Journal of neuropathology and experimental neurology* **49**, 215-224 (1990).

7. Selden, N., Mesulam, M.M. & Geula, C. Human striatum: the distribution of neurofibrillary tangles in Alzheimer's disease. *Brain Res* **648**, 327-331 (1994).

8. Hanseeuw, B.J., *et al.* PET staging of amyloidosis using striatum. *Alzheimers Dement* **14**, 1281-1292 (2018).

9. Beach, T.G., *et al.* Striatal amyloid plaque density predicts Braak neurofibrillary stage and clinicopathological Alzheimer's disease: implications for amyloid imaging. *J Alzheimers Dis* **28**, 869-876 (2012).

10. Hanseeuw, B.J., *et al.* Striatal amyloid is associated with tauopathy and memory decline in familial Alzheimer's disease. *Alzheimers Res Ther* **11**, 17 (2019).

11. Li, W., Avram, A.V., Wu, B., Xiao, X. & Liu, C. Integrated Laplacian-based phase unwrapping and background phase removal for quantitative susceptibility mapping. *NMR Biomed* **27**, 219-227 (2014).

12. Thomas, B.A., *et al.* PETPVC: a toolbox for performing partial volume correction techniques in positron emission tomography. *Phys Med Biol* **61**, 7975-7993 (2016).

13. Labbe, C., Froment, J.C., Kennedy, A., Ashburner, J. & Cinotti, L. Positron emission tomography metabolic data corrected for cortical atrophy using magnetic resonance imaging. *Alzheimer Dis Assoc Disord* **10**, 141-170 (1996).

14. Thomas, B.A., *et al.* The importance of appropriate partial volume correction for PET quantification in Alzheimer's disease. *Eur J Nucl Med Mol Imaging* **38**, 1104-1119 (2011).

15. Langley, J., Hussain, S., Flores, J.J., Bennett, I.J. & Hu, X. Characterization of age-related microstructural changes in locus coeruleus and substantia nigra pars compacta. *Neurobiol Aging* **87**, 89-97 (2020).

16. Wadhwani, A.R., Affaneh, A., Van Gulden, S. & Kessler, J.A. Neuronal apolipoprotein E4 increases cell death and phosphorylated tau release in alzheimer disease. *Ann Neurol* **85**, 726-739 (2019).